

## Challenges in Forming Millisecond Pulsar–Black Holes from Isolated Binaries

CAMILLE LIOTINE,<sup>1,2</sup> VICKY KALOGERA,<sup>1,2,3</sup> JEFF J. ANDREWS,<sup>4,5</sup> SIMONE S. BAVERA,<sup>6,7</sup> MAX BRIEL,<sup>6,7</sup>  
TASSOS FRAGOS,<sup>6,7</sup> SETH GOSSAGE,<sup>2,3</sup> KONSTANTINOS KOVLAKAS,<sup>8,9</sup> MATTHIAS U. KRUCKOW,<sup>6,7</sup> KYLE A. ROCHA,<sup>1,2,3</sup>  
PHILIPP M. SRIVASTAVA,<sup>10,2,3</sup> MENG SUN,<sup>2</sup> ELIZABETH TENG,<sup>1,2,3</sup> ZEPEI XING,<sup>6,7</sup> AND EMMANOUIL ZAPARTAS<sup>11</sup>

<sup>1</sup>*Department of Physics and Astronomy, Northwestern University, 2145 Sheridan Road, Evanston, IL 60208, USA*

<sup>2</sup>*Center for Interdisciplinary Exploration and Research in Astrophysics (CIERA), Northwestern University, 1800 Sherman Ave, Evanston, IL 60201, USA*

<sup>3</sup>*NSF-Simons AI Institute for the Sky (SkAI), 172 E. Chestnut St., Chicago, IL 60611, USA*

<sup>4</sup>*Department of Physics, University of Florida, 2001 Museum Rd, Gainesville, FL 32611, USA*

<sup>5</sup>*Institute for Fundamental Theory, 2001 Museum Rd, Gainesville, FL 32611, USA*

<sup>6</sup>*Département d’Astronomie, Université de Genève, Chemin Pegasi 51, CH-1290 Versoix, Switzerland*

<sup>7</sup>*Gravitational Wave Science Center (GWSC), Université de Genève, CH1211 Geneva, Switzerland*

<sup>8</sup>*Institute of Space Sciences (ICE, CSIC), Campus UAB, Carrer de Magrans, 08193 Barcelona, Spain*

<sup>9</sup>*Institut d’Estudis Espacials de Catalunya (IEEC), Edifici RDIT, Campus UPC, 08860 Castelldefels (Barcelona), Spain*

<sup>10</sup>*Electrical and Computer Engineering, Northwestern University, 2145 Sheridan Road, Evanston, IL 60208, USA*

<sup>11</sup>*Institute of Astrophysics, Foundation for Research and Technology-Hellas, GR-71110 Heraklion, Greece*

Submitted to ApJ

### ABSTRACT

Binaries harboring a millisecond pulsar (MSP) and a black hole (BH) are a key observing target for current and upcoming pulsar surveys. We model the formation and evolution of such binaries in isolation at solar metallicity using the next-generation binary population synthesis code POSYDON. We examine neutron star (NS)–BH binaries where the NS forms first (labeled NSBH), as the NS must be able to spin-up to MSP rotation periods before the BH forms in these systems. We find that NSBHs are very rare and have a birth rate  $< 1 \text{ Myr}^{-1}$  for a Milky Way-like galaxy in our typical models. The NSBH formation rate is 2–3 orders of magnitude smaller than that for NS–BHs where the BH forms first (labeled BHNS). These rates are also sensitive to model assumptions about the supernova (SN) remnant masses, natal kicks, and common-envelope (CE) efficiency. We find that 100% of NSBHs undergo a mass ratio reversal before the first SN and up to 64% of NSBHs undergo a double common envelope phase after the mass ratio reversal occurs. Most importantly, no NSBH binaries in our populations undergo a mass transfer phase, either stable or unstable, after the first SN. This implies that there is no possibility of pulsar spin-up via accretion, and thus MSP–BH binaries cannot form. Thus, dynamical environments and processes may provide the only formation channels for such MSP–BH binaries.

### 1. INTRODUCTION

Pulsars are highly magnetized, rapidly rotating NSs most commonly detectable as radio sources. Some pulsars get “recycled” during their lifetime via accretion, which causes them to spin-up to shorter rotation periods. If they reach periods  $\lesssim 30 \text{ ms}$ , this places them in the distinct category of MSPs (see Phinney & Kulkarni 1994; Lorimer 2008; D’Antona & Tailo 2020, for reviews).

Detecting a Galactic pulsar–BH binary is an observation goal for current and upcoming pulsar surveys, such as the ongoing MeerKAT (Booth et al. 2009), FAST (Nan et al. 2011), and CHIME (Stairs 2019; Amiri

et al. 2021) surveys, as well as surveys with the upcoming Square Kilometer Array (Braun et al. 2019). Observing a pulsar–BH binary would enable unprecedented tests of general relativity due to the extreme curvature of spacetime around the system (e.g., Kramer et al. 2004; Seymour & Yagi 2018). A MSP–BH detection is of particular interest because the short MSP pulse periods provide the timing precision necessary to measure the Shapiro delay (the signal delay resulting from light passing a massive object), which can provide additional constraints on the NS mass and equation of state (Shapiro 1964; Fonseca et al. 2019). In addition, MSPs can exist as detectable sources for over ten times longer than regular pulsars and have wider beams due

to their short pulse periods, both of which increase their overall detection probability (e.g., Lorimer 2008).

A recent observation made with the MeerKAT telescope has identified a MSP in a binary with a compact object (CO) in the lower mass gap between the heaviest NSs and the lightest BHs (Barr et al. 2024). Located in the globular cluster (GC) NGC 1851, this system is thought to have formed dynamically (Barr et al. 2024); the MSP was spun-up by a low-mass companion that was later replaced by a high-mass companion in an exchange interaction. The lack of radio detections of the high-mass companion makes it impossible to distinguish between a high-mass NS and low-mass BH (Barr et al. 2024).

Many studies have predicted how MSP–BH binaries, as well as NS–BH binaries more broadly, could form dynamically in GCs (e.g., Clausen et al. 2014; Ye et al. 2019a,b; Arca Sedda 2020; Fragione & Banerjee 2020). While it is known that GCs are very efficient at forming MSPs compared to the Galactic field due to their high stellar densities (e.g., Manchester et al. 2005; Ransom 2008; Bahramian et al. 2013), GCs are relatively inefficient at forming NS–BH binaries (Clausen et al. 2013; Ye et al. 2019a; Arca Sedda 2020; Hoang et al. 2020), and the number of MSPs may even be anti-correlated with the number of BHs in a given cluster (Ye et al. 2019b). In this study, we focus on the formation of isolated MSP–BH binaries in the Galactic field and thus do not examine the possible dynamical formation channels of these systems.

Many binary population synthesis (BPS) studies have previously examined isolated NS–BH formation with a focus on their properties as gravitational wave (GW) sources (Kruckow et al. 2018; Mapelli & Giacobbo 2018; Shao & Li 2018; Broekgaarden et al. 2021; Chattopadhyay et al. 2021; Román-Garza et al. 2021; Drozda et al. 2022; Xing et al. 2023, 2024). Growing interest in this area of research is related to the GW detections consistent with being the products of NS–BH coalescences that have been recently reported by the LIGO–Virgo–KAGRA (LVK) collaboration. Their connection to multi-messenger astronomy as potential gamma-ray burst and kilonovae sources is also of particular interest (see e.g., Mészáros et al. 2019; Branchesi 2023, for reviews).

The events GW200115 and GW230529 were both reported with high confidence and with estimated component masses consistent with NS–BH binaries (Abbott et al. 2021; Abac et al. 2024). However, the most massive (primary) component for GW230529 was estimated between 2.5–4.5  $M_{\odot}$ , and one cannot rule out that it was a massive NS. GW190814 was also reported with

high confidence, with primary and secondary masses of  $23.3^{+1.4}_{-1.4}$  and  $2.6^{+1}_{-1}$   $M_{\odot}$ , respectively (Abbott et al. 2020, 2024). Given the high secondary mass and the absence of additional tidal measurements or electromagnetic counterparts, it remains unclear whether GW190814 originated from a NS–BH or BH–BH coalescence. GW200210 was detected with a similar secondary mass of  $2.83^{+0.47}_{-0.42}$   $M_{\odot}$  but a lower probability of astrophysical origin of 0.54 (Abbott et al. 2023). GW191219 and GW190917 were reported with component masses consistent with NS–BH binaries, but with uncertain probabilities of astrophysical origin due to systematics (Abbott et al. 2023, 2024). Finally, GW190426\_152155 and GW200105 were reported as marginal candidates with masses consistent with NS–BH binaries but low probability ( $< 0.5$ ) of astrophysical origin (Abbott et al. 2021, 2023, 2024).

In this paper, we use the POSYDON population synthesis code (Fragos et al. 2023; Andrews et al. 2024) to examine the possible formation channels of isolated Galactic NS–BH binaries that host recycled NSs, regardless of whether they become potential GW sources or not. As previously mentioned, the NSs in these binaries are expected to form first so that they may accrete from their companions and be spun-up before the BH forms. Past BPS studies have examined such binaries in detail, including Kruckow et al. (2018) and Chattopadhyay et al. (2021), but come to opposing conclusions regarding their presence in Milky Way-like galaxies. We discuss our detailed results in conversation with these findings in Section 4.1.

In Section 2, we discuss our BPS models and the POSYDON code. In Section 3, we discuss the properties of NS–BH binaries in our BPS populations, including their birth rates, formation channels, and double compact object (DCO) properties. In Section 4, we place our findings in the context of previous studies as well as current and future MSP–BH detections, in addition to discussing our model uncertainties. In Section 5, we summarize our conclusions.

## 2. METHODS

We generate populations of  $10^7$  binaries at solar metallicity ( $Z = 0.0142$ ) with Version 2 of the BPS code POSYDON (Andrews et al. 2024). POSYDON is unique from other BPS codes in that it uses detailed grids of stellar and binary models generated using MESA (Paxton et al. 2011, 2013, 2015, 2019) to self-consistently evolve the binary components’ stellar structure with the binary evolution. For a detailed description of the code, see Fragos et al. (2023) and Andrews et al. (2024).

### 2.1. Binary Population Models

We use POSYDON’s initial-final interpolation scheme (Fragos et al. 2023; Andrews et al. 2024) to acquire binary properties from the grids of pre-computed models in all of our populations. This scheme first classifies binaries being evolved with a given MESA grid into a mass transfer (MT) history class for that grid based on the binary component masses and orbital period. Then, the physical properties of the binaries are interpolated from the grid values within each MT class (Fragos et al. 2023; Andrews et al. 2024).

The BPS initial conditions are as follows: We draw primary masses using the initial mass function (IMF) from Kroupa (2001) and initial binary orbital periods using the prescription detailed in Sana et al. (2012). Primary masses are in the range  $6.2\text{--}120 M_{\odot}$  and secondary masses are in the range  $0.35\text{--}120 M_{\odot}$  to align with the mass ranges of POSYDON’s pre-computed binary grids. We sample secondary masses assuming an initially flat mass ratio distribution. We apply a burst star formation history, which assumes all stars are formed at the same time, and evolve our binaries for 13.8 Gyr. We obtain astrophysical results by renormalizing to a constant star formation rate.

We make several additional modeling assumptions, detailed below, including those that affect POSYDON’s “on-the-fly” calculations for stages of evolution not handled by the pre-calculated MESA grids.

#### 2.2. Mass Transfer

All MT in POSYDON is handled within the pre-computed MESA grids of binary models, and thus MT settings cannot be changed without running new grids. We briefly describe how different MT cases are treated in the standard POSYDON grids used for this study. For full details, refer to Fragos et al. (2023) and Andrews et al. (2024).

Mass-loss due to Roche-lobe overflow (RLO) of main-sequence (MS) stars is handled using the `contact` scheme within MESA. This prescription is suitable for modeling the structure of MS binary evolution, including cases in which one or both stars overflow their Roche lobes. When stars evolve off the MS, modeling is switched to the `Ko1b` scheme (Kolb & Ritter 1990), which more accurately handles stars with expanded envelopes.

POSYDON Version 2 also includes treatment for reverse MT, which occurs when a MT phase from the primary to the secondary takes place and afterwards the secondary initiates “reverse” MT back onto the primary. This happens frequently in regions of parameter space where the zero-age main-sequence (ZAMS) mass ratio of

the binary is close to one. Reverse MT is not traditionally supported by the `Ko1b` scheme, and thus modifications were made to the MESA code used to run POSYDON’s pre-calculated grids that enable the switching of donors when the MT rate from the secondary exceeds that of the primary (Andrews et al. 2024).

Mass accretion is handled differently depending on the accretor type. For binaries with a non-degenerate accretor, all the mass lost by the donor through RLO is initially accepted by the accretor. This spins-up the accreting star as long as it has not reached a critical rotation rate. In the case of critically-rotating stars, accretion is restricted and mass will begin to be ejected by the binary through isotropic stellar winds. The wind mass-loss rate of the accretor is calculated with a rotationally-enhanced wind model that boosts stellar winds to ensure the stellar rotation rate always remains below its critical threshold (Fragos et al. 2023). The overall effect of these assumptions is that the mass accretion may be highly inefficient depending on the accretor’s angular momentum and stellar structure, even when enforcing that all mass lost from the donor is initially transferred to the accretor during RLO. While boosted winds are commonly used to model these systems (e.g., Paxton et al. 2013), star-disk interactions also play a crucial role in the accretor spin-up. Improved understanding of star-disk interactions could change the spin-up and accretion assumptions for rapidly-rotating stars (Colpi et al. 1991; Paczynski 1991; Popham & Narayan 1991).

For binaries with degenerate accretors, MT proceeds similarly except that it is Eddington-limited; sub-Eddington MT rates are conservative, and super-Eddington rates cause excess matter to be lost via an isotropic wind from the vicinity of the accretor. For full details on how the Eddington-limited accretion rate is calculated, refer to Fragos et al. (2023)

#### 2.3. Common-Envelope Evolution

If a binary experiences dynamically unstable MT, it can undergo CE evolution (Paczynski 1976; Ivanova et al. 2020). POSYDON determines the onset of an unstable MT phase using various criteria in its pre-computed grids of binary models. First, if the MT rate of the binary exceeds  $0.1 M_{\odot} \text{ yr}^{-1}$ , the binary is assumed to enter an unstable RLO phase. The binary will also begin unstable MT if the stellar radius of the expanding star extends beyond the gravitational equipotential surface, or second Lagrangian point  $L_2$ . For CO accretors, a CE phase is assumed to begin if the accretor’s photon-trapping radius reaches its Roche-lobe radius. Lastly, if both stars in the binary fill their Roche-lobes while at least one of the stars is in a post-MS phase of evolu-

tion, the binary is assumed to initiate unstable MT. For full details on these assumptions, refer to [Fragos et al. \(2023\)](#).

We treat CE as an instantaneous process using the standard  $\alpha - \lambda$  formalism ([Webbink 1984](#); [Livio & Soker 1988](#)), where  $\alpha$  is the CE efficiency parameter and  $\lambda$  is the envelope binding energy factor. We set  $\alpha = 1$  for the efficiency parameter in our default models, but also examine model variations with  $\alpha = 0.5$  and  $\alpha = 0.1$  in Section 3.4.2. For the binding energy factor, POSYDON is able to self-consistently calculate  $\lambda$  at the onset of CE using the stellar profiles from the pre-calculated binary grids. To define the core-envelope boundary, we assume a hydrogen (H) abundance fraction and a helium (He) abundance fraction of 0.1. If a CE ejection is successful, we assume that that core mass and radius of the star are the same as before the CE began, rather than being set by the H and He abundance fractions. We assume that Hertzsprung-Gap donor stars are able to undergo and survive a CE phase, which is commonly referred to as the “optimistic” CE scenario in the literature (e.g., [Vigna-Gómez et al. 2018](#)).

POSYDON also includes treatment for double CE evolution. This occurs when both stars in the binary have overfilled their Roche-lobes and both have a giant-like structure with a distinct core-envelope separation. In addition, unstable MT must have been initiated by at least one star in the binary. In this case,  $\lambda$  is calculated separately for both stars ( $\lambda_1, \lambda_2$ ) and the binding energy for each is summed to get the total binding energy:

$$E_{\text{bind}} = -G \left[ \frac{m_1(m_1 - m_{1,c})}{\lambda_1 R_1} + \frac{m_2(m_2 - m_{2,c})}{\lambda_2 R_2} \right] \quad (1)$$

where  $m_i$ ,  $m_{i,c}$ , and  $R_i$  are the total stellar mass, core mass, and stellar radius of the  $i$ -th component of the binary, respectively. The orbital energy and separation of the binary after the double CE are then calculated using  $E_{\text{bind}}$  like in the single CE case ([Fragos et al. 2023](#)).

Though the modeling of double CE is uncertain, there is observational evidence indicating that this process does occur in nature ([Ahmad et al. 2004](#); [Justham et al. 2011](#); [Şener & Jeffery 2014](#)). The conditions for the onset of a double CE are thought to differ from those for a single CE because *both* stars in a double CE binary have well-developed cores with extended envelopes (in the traditional single CE treatment, one star is expected to have this structure while the other object is assumed to be dense). This implies that the stars have comparable masses, in which case MT is not expected to become dynamically unstable as a direct consequence of RLO or tidal instability ([Ivanova et al. 2020](#)). There also may be additional methods of initiating unstable MT partic-

ular to these binaries that would require expensive 3D hydrodynamical simulations to understand, which has not yet been done ([Ivanova et al. 2020](#)). Thus, it is uncertain how many binaries whose stars meet our double CE requirements actually initiate unstable MT and reach orbital instability, and of these binaries, which will undergo a successful double CE phase and which will merge.

#### 2.4. Core Collapse

The model used to calculate the remnant masses of COs formed from the core collapse of massive stars significantly impacts the NS and BH mass distributions in binary populations. We model binary populations using the “delayed” prescription from [Fryer et al. \(2012\)](#) as well as the “N20” engine prescription from [Sukhbold et al. \(2016\)](#), as these are two prescriptions in POSYDON that allow for the formation of BHs in the low-end mass gap (3–5  $M_{\odot}$ ). This is important to consider given the recent observational evidence of BHs existing in this gap ([Abac et al. 2024](#)). The Fryer–12–delayed (F12d) model uses the carbon-oxygen (C–O) core mass of the star at the start of the core-collapse (CC) as well as the amount of fallback material onto the proto-CO after the explosion to determine the final baryonic mass of the CO. This prescription also uses a maximum NS mass limit to determine the remnant type (NS or BH), which we set to 2.5  $M_{\odot}$ . The Sukhbold–16 (S16) model uses the He core mass of the star prior to its collapse to determine both the remnant mass and fallback onto the CO as well as its remnant type.

Stars with ZAMS masses in the range  $\sim 7$ –10  $M_{\odot}$  may undergo an electron-capture supernova (ECSN) when they have degenerate ONeMg cores, producing less-energetic explosions and hence smaller SN kicks (e.g., [Nomoto 1984](#); [Podsiadlowski et al. 2004](#); [Hiramatsu et al. 2021](#)). For ECSNe, we model binary populations using the prescription from [Podsiadlowski et al. \(2004\)](#). With this formalism, pre-CC stars with core He masses between 1.4–2.5  $M_{\odot}$  will undergo an ECSN.

Stars that have lost their surface layers during binary interactions may undergo an ultra-stripped supernova (USSN) and will receive smaller natal kicks than in a core-collapse supernova (CCSN) (e.g., [Tauris et al. 2015](#)). POSYDON currently does not include treatment for USSNe. However, we do not expect this to affect our main results, as past studies have shown that USSNe primarily occur in NS–BH binaries where the BH forms first ([Chattopadhyay et al. 2021](#)).

To model the kicks of newly-born COs formed from CCSNe, we sample kicks from a Maxwellian distribution with a velocity dispersion of 265 km s<sup>−1</sup> ([Hobbs et al.](#)

**Table 1.** Birth rates ( $\text{Myr}^{-1}$ ) of NSBH, BHNS, and combined NS–BH binaries in a Milky Way-like galaxy for all of our population models.

Model	NSBH	BHNS	NS–BH
F12d	0.05	36.35	36.40
S16	0.63	63.90	64.53
F12d, low $\sigma_{\text{CCSN}}$	0.30	125.31	125.61
S16, low $\sigma_{\text{CCSN}}$	1.61	174.63	176.24
S16, $\alpha = 0.5$	0.24	55.39	55.63
S16, $\alpha = 0.1$	0.19	50.95	51.14

2005). For the kicks of NSs formed from ECSNe, we use a velocity dispersion of  $20 \text{ km s}^{-1}$  (Giacobbo & Mapelli 2019). We also investigate one model variation with reduced CCSNe kicks, designated as “low  $\sigma_{\text{CCSN}}$ ”, that uses the velocity dispersion estimates from Mandel & Müller (2020). This study applies the results from three-dimensional supernova simulations and semi-analytical parameterized models to derive stochastic prescriptions for the natal kicks of NSs and BHs. They estimate that the scatter for NS kicks is  $\sim 120 \text{ km s}^{-1}$  and the scatter for BH kicks is  $\sim 60 \text{ km s}^{-1}$ . They acknowledge that these estimates under-predict kick velocities for the least-massive C–O cores ( $\lesssim 4 M_{\odot}$ ) compared to detailed semi-analytic predictions due to uncertainties in stellar evolution and explosion models (Mandel & Müller 2020). For this reason, we consider their kick scatter estimates to be a lower-limit for natal kicks, particularly for NSs formed from low-mass C–O cores.

As in the default POSYDON treatment, we normalize all BH kicks by multiplying by  $1.4 M_{\odot}$  and dividing by the remnant mass in order to approximately rescale the NS kick distribution to one suited for heavier COs (Fragos et al. 2023).

### 3. RESULTS

We examine the subpopulations of NS–BH binaries in which the NS forms first (NSBHs) in contrast to those where the BH forms first (BHNSs). We focus on the properties and evolution of NSBH binaries, as we are interested in their relation to MSP–BH systems in which it is necessary for the NS to form first so that it has the chance to be spun-up to millisecond rotation periods before BH formation.

#### 3.1. Frequency of NS–BH Binaries

We calculate the birth rates of NSBHs and BHNSs in a Milky Way-like galaxy to understand their relative frequencies in our populations (Table 1). We cal-

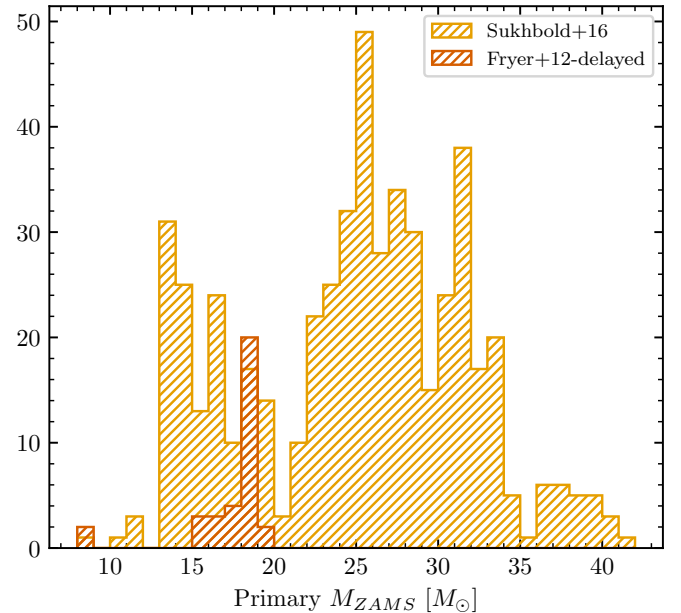


**Figure 1.** The primary ZAMS masses of all NSBH progenitors in our S16 and F12d populations. The differing mass ranges between prescriptions is a result of how each computes remnant masses and assigns CO types (Section 3.1).

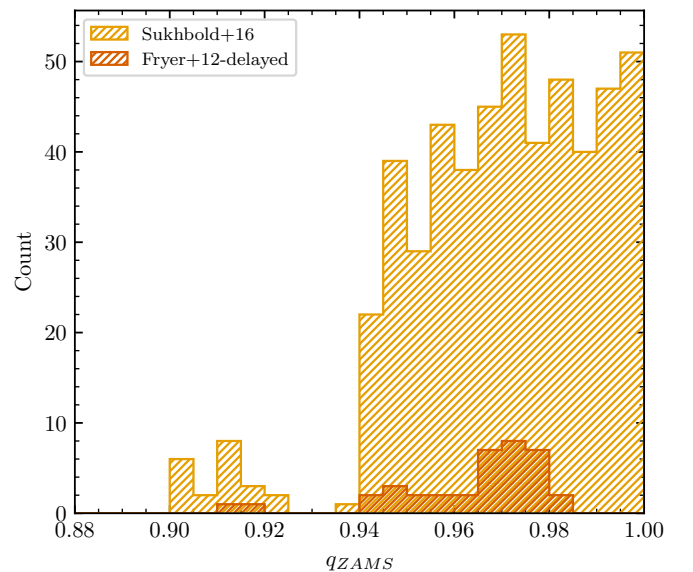


**Figure 2.** The mass ratio distributions at ZAMS ( $q_{\text{ZAMS}}$ ) for all NSBH progenitors. In both the F12d and S16 populations, the ZAMS mass ratios are close to unity.

culate birth rates by rescaling the number of binaries in a given subpopulation with the average star formation rate of the Milky Way, which we take to be  $\text{SFR}_{\text{MW}} = 1.65 M_{\odot}/\text{yr}$  (Licquia & Newman 2015). We normalize our simulations by: multiplying the number of systems

by  $\text{SFR}_{MW}$  and dividing by the total underlying mass of the POSYDON population, which is the stellar mass of the population at ZAMS after integrating the associated population IMF and period distribution fully. Our NS–BH birth rates are order-of-magnitude comparable with those calculated by Chattopadhyay et al. (2021).

In most of our POSYDON models, we find that the birth rate of bound NSBH binaries, including systems that do and do not merge in a Hubble time, is  $< 1 \text{ Myr}^{-1}$ . In all of our populations, the birth rate of NSBH binaries is 2–3 orders of magnitude smaller than that for BHNS binaries. This is to be expected, as BHs tend to form from heavier stellar primaries that evolve more quickly than their lighter secondary counterparts. The high prevalence of BHNSs compared to NSBHs is in agreement with previous BPS studies that examine NS–BH populations (e.g., Kruckow et al. 2018; Chattopadhyay et al. 2021; Xing et al. 2023).

When comparing the birth rates of NSBHs in the F12d vs. the S16 populations, we find that there are about 10 times more NSBHs in the S16 population, and the total NS–BH rate increases by  $\lesssim 2$ . This is a result of differences in how remnant masses are determined in the F12d and S16 prescriptions.

The S16 SN mechanism, exploded with the N20 engine in our populations, produces CO remnant types in a relatively stochastic manner. In Sukhbold et al. (2016), they find that N20 models with ZAMS stellar masses up to  $120 M_{\odot}$  can successfully explode and form NS remnants, while models with ZAMS masses as low as  $\sim 15 M_{\odot}$  can implode to form BH remnants (not taking into account binary interactions that may change the stellar mass before collapse). The primary ZAMS mass parameter space for our NSBH binaries in the S16 population falls between  $10\text{--}40 M_{\odot}$  (Figure 1) and the secondary masses fall in a similar range, as all NSBHs have ZAMS mass ratios close to one (Figure 2, see 3.2 and 4.1 for discussion). The remnant types produced for stars with primary ZAMS masses between  $15\text{--}40 M_{\odot}$  switches frequently between BHs and NS in the S16 treatment (Sukhbold et al. 2016). Thus, stars with higher initial masses can end-up producing NS remnants, and those with lower initial masses can produce BH remnants, which constructs a wider parameter space for possible NSBH formation.

The F12d mechanism functions differently, as it determines the remnant CO type using the maximum NS mass limit, which we set to  $2.5 M_{\odot}$ . The remnant mass itself is determined using the C–O core mass of the progenitor star at the time of explosion, which is related to the mass of the star at ZAMS (Fryer et al. 2012). Because all NSBH progenitors have ZAMS mass ratios

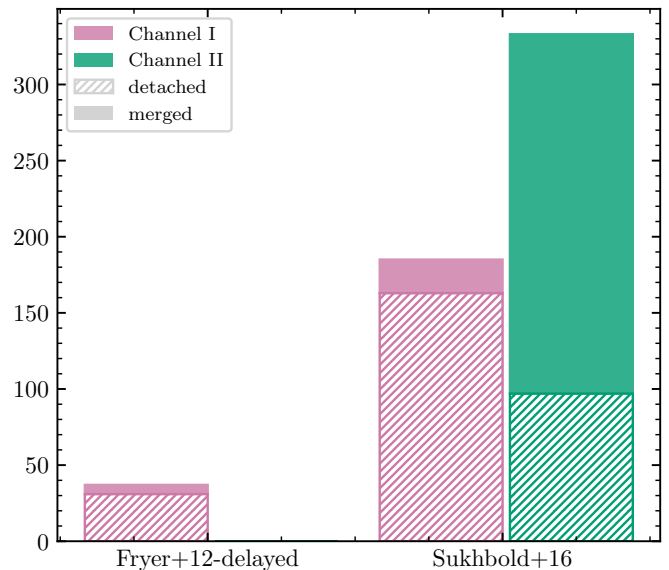


**Figure 3.** The number of NSBH binaries in the F12d and S16 populations that form through Channel I (pink) vs. Channel II (green) (Sections 3.2.2 & 3.2.3). We show the subset of binaries in each channel that merge in a Hubble time (solid) and those that do not merge, or remain detached (hatched).

close to one (Section 3.2, Figure 2), this implies that, when evolved with the F12d prescription, they are only likely to have masses that fall in the necessary range for becoming high-mass NSs or low-mass BHs. This range corresponds to ZAMS masses between  $\sim 15\text{--}20 M_{\odot}$  according to the results in Fryer et al. (2012). Indeed, we find that 86% of the NSBHs in the F12d population have primary ZAMS masses in this range (Figure 1). Because the parameter space for possible NSBH formation is narrower in the F12d treatment, much fewer NSBHs will form in a given population.

### 3.2. NSBH Formation Channels

As previously mentioned, all NSBH progenitors in our populations have ZAMS mass ratios ( $q = M_2/M_1$ ) close to unity ( $\gtrsim 0.9$ ) as shown in Figure 2. We find that binaries with ZAMS mass ratios down to  $\sim 0.4$  can have primaries that form NSs and secondaries that form BHs, but they get disrupted at the first SN and thus do not contribute to our NSBH populations.

Having ZAMS mass ratios close to one also makes it easier for these systems to undergo a mass ratio reversal (in which the secondary object becomes heavier than the primary) before the first SN, which increases the possibility of NS formation occurring before BH formation depending on the SN prescription and ZAMS mass values. We find that 100% of NSBH progenitors in both our S16 and F12d populations have a heavier secondary

star than primary star before the first SN due to MT during their hydrogen main-sequence (HMS–HMS) evolution (Sections 3.2.1 and 4.1).

We find that NSBH binaries form via two different channels after the HMS–HMS phase. The first channel, designated as Channel I, has fully detached evolution of the binary components after the HMS–HMS phase. In the second channel, designated as Channel II, the binaries undergo a double CE phase immediately after the HMS–HMS phase and before the first SN. The breakdown of how many binaries form through each channel in each population, including binaries that do and do not merge in a Hubble time, is shown in Figure 3. We discuss these two different channels in detail in Sections 3.2.2 & 3.2.3.

### 3.2.1. Mass Transfer Before First SN

We examine the MT history before a possible double CE is triggered and before the first SN by looking at the HMS–HMS MESA grid slices from POSYDON’s library of binary star models. The HMS–HMS grids summarize the evolution of binaries with two stars at ZAMS until they reach a designated stopping condition in MESA (Fragos et al. 2023; Andrews et al. 2024). Each grid is computed for a range of initial primary masses ( $M_1$ ), orbital periods ( $P_{\text{orb}}$ ), and mass ratios ( $q$ ). An example of these grid slices overlaid with the ZAMS primary masses and orbital periods of the S16 NSBH progenitors is shown in Figure 4. We only show the S16 population here because the F12d population has far fewer NSBH binaries and their progenitors fall in similar regions on the HMS–HMS grids as the S16 NSBH binaries.

The different grid symbols, or “termination flags”, summarize the evolution of each of the pre-computed MESA models. The cyan star and blue triangle markers plotted on top of the grids represent the NSBH progenitors in our S16 BPS population and distinguish between NSBHs that do and do not merge in a Hubble time, respectively. NSBH binaries with initial mass ratios  $\leq 0.95$  are plotted on the  $q = 0.9$  grid slice, while those with mass ratios  $> 0.95$  are plotted on the  $q = 1.0$  grid slice. This division exists for plotting purposes only, as POSYDON interpolates discrete grid values to get the MT class and evolution of each binary with its unique  $q$ ,  $P_{\text{orb}}$ , and  $M_1$ .

Looking at Figure 4, we see that all NSBH progenitors undergo MT before the first SN occurs. The termination flags with diamond markers represent models that ended their HMS–HMS evolution by triggering a CE event, while square markers indicate that one of the stars completed its evolution by reaching core carbon depletion. The marker colors differentiate the evolutionary

state of the donor star when the latest MT phase was initiated, ranging from MS (blue) to post-MS (tan) to stripped He–MS (brown). The green markers indicate that reverse MT occurred (Section 2.2). Orange markers indicate that the binary underwent a contact phase where both stars filled their Roche lobes simultaneously at some point during the HMS–HMS evolution. The orange diamond markers specifically indicate that the binary terminated its HMS–HMS evolution by triggering a double CE event.

Many of the NSBHs on the  $q = 1.0$  grid fall near the boundary between the reverse MT (green) and contact (orange) MT classes. The most important consequence of this is that a given binary’s probability of entering (double) CE before the first SN relies heavily on POSYDON’s classification of its HMS–HMS MT class around the class boundary, and thus it may be somewhat uncertain. However, because we find that all NSBH progenitors experience a mass-ratio reversal before the first SN regardless of the specific type of MT that occurred, we do not expect this uncertainty to greatly impact our results apart from the prevalence of double CE NSBH formation, which impacts the NSBH orbital period-eccentricity distribution at DCO formation (Section 3.3) and the overall NSBH birth rate (Section 3.4.2).

We see that most binaries on the  $q = 0.9$  grid fall in the stable regions of evolution (square markers) and do not enter CE before the first SN, but many on the  $q = 1.0$  grid fall in regions that enter a double CE (diamond markers) before the first SN. This difference in evolution distinguishes the Channel I and Channel II formation pathways for NSBHs discussed in Sections 3.2.2 & 3.2.3. We find that all of the NSBH progenitors on the  $q = 1.0$  grid with ZAMS orbital periods  $\gtrsim 40$  days and primary mass  $\gtrsim 25 M_{\odot}$  (upper right region of NSBHs) enter a double CE after the HMS–HMS step, following the Channel II path of evolution. The majority ( $\sim 71\%$ ) of these binaries merge in a Hubble time (cyan markers). This is expected, as the double CE phase significantly tightens the binary orbit and facilitates merging on shorter timescales (Section 3.2.3).

### 3.2.2. Channel I: Fully Detached Evolution

In Channel I for forming NSBHs, the binary evolution is fully detached after the HMS–HMS phase. We find that 100% of the NSBHs in the F12d population and 36% of the NSBHs in the S16 population form through this channel. No MT occurs in these binaries after the first SN. In particular, there is no Case BB MT (where the donor is undergoing He-shell burning during RLO), which is thought to be necessary to spin-up pulsars with future NS or white dwarf companions to MSP

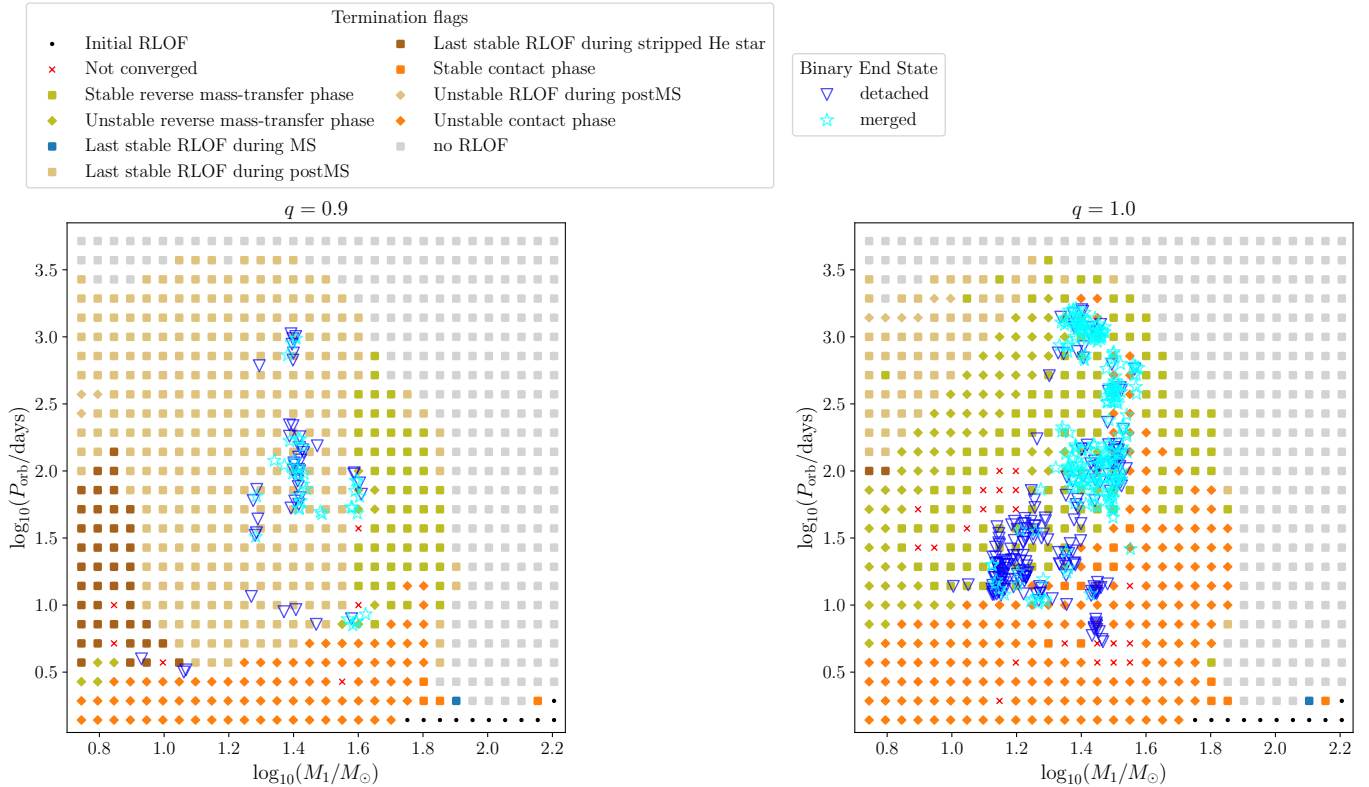


**Figure 4.** The HMS–HMS grid slices from POSYDON’s library of binary star models for ZAMS mass ratios  $q = 0.9$  and  $q = 1.0$ . The different grid symbols summarize the evolution of each of the pre-computed MESA models. The ZAMS binary orbital periods vs. primary masses for all NSBH progenitors in the S16 BPS population are plotted over the grids, where the cyan star and blue triangle markers distinguish between binaries that do and do not merge in a Hubble time, respectively. Binaries with initial mass ratios  $\leq 0.95$  are potted on the  $q = 0.9$  grid slice, while those with mass ratios  $> 0.95$  are plotted on the  $q = 1.0$  grid slice.

speeds (Tauris et al. 2012; Lazarus et al. 2014; Tauris et al. 2017). Channel I NSBHs also do not experience any CE evolution after the first SN, so there is no possibility for unstable MT onto the NS to occur during CE.

The lack of stable MT arises from the fact that the He-burning stellar progenitors of BHs in our NSBH populations are too heavy to expand and fill their Roche lobes. All of their He core masses before the second SN are  $> 4 M_{\odot}$ , and many are much heavier, with masses of 10–11  $M_{\odot}$ . He-burning stars with core masses  $\gtrsim 4 M_{\odot}$  can have radii up to two orders of magnitude smaller than He-burning stars with lighter core masses (Habets 1986). In addition, a CE phase traditionally helps to shrink the binary orbit, making it easier for these heavy stars to initiate RLO, but CE is not triggered after the first SN in these binaries (for more discussion on why CE does not occur, refer to Section 4.1).

We find that 99% of NSBH progenitors in our S16 population and 81% of NSBH progenitors in our F12d population have companion stars on the He–MS or post He–MS immediately following the HMS–HMS stage of evolution when the primary has formed a NS. The remain-

ing NSBH progenitors have companions that are H-rich stars undergoing H-core or H-shell burning. The binaries with H-core burning companions have wide orbital periods ( $> 150$  days) that prevent them from undergoing RLO. The binaries with H-shell burning companions have shorter orbital periods ( $< 20$  days), but most of them already underwent stable reverse MT (where the secondary transfers mass to the primary) during the HMS–HMS evolution. Thus, RLO from the secondary companion already occurred before the NS formation, preventing accretion onto the NS.

The breakdown of how many NSBHs formed through Channel I that do and do not merge in a Hubble time is shown in Figure 3. We see that most binaries remain detached, which is due to the fact that there is no mechanism such as (double) CE to help tighten the binary orbit. We find that only 16% of NSBHs in the F12d population and 12% of NSBHs in the S16 population merge in a Hubble time if formed through Channel I. Most of the binaries that do merge have very high eccentricities ( $> 0.9$ ) upon DCO formation (Figure 6), which allows them to merge on shorter timescales (Peters 1964).



### 3.2.3. Channel II: Double CE Evolution

In Channel II, NSBH progenitors undergo a double CE after the HMS–HMS phase of evolution and before the first SN. Channel II dominates the NSBH formation in the S16 population, accounting for 64% of its NSBHs. No NSBHs form through this channel in the F12d population. This is because these binaries have primary masses  $\lesssim 20 M_{\odot}$  at ZAMS, and thus they are not massive enough to fall inside the region of the HMS–HMS grids where binaries undergo a double CE. The double CE region is located at  $P_{\text{orb}} \gtrsim 40$  days and  $M_1 \gtrsim 25 M_{\odot}$  in the  $q = 1.0$  grid of Figure 4.

The main difference between the NSBH populations formed through this channel vs. Channel I is that there is a higher fraction of merging NSBHs in Channel II. About 71% of NSBHs formed through Channel II in the S16 population merge in a Hubble time (Figure 3). This is because the double CE phase tightens the binary orbit, which greatly facilitates the ability to merge on shorter timescales. We find that all NSBHs formed through Channel II have orbital periods  $< 0.5$  days after the double CE phase, even though 87% of them start with orbital periods  $> 100$  days before the double CE begins. The reason that these binaries go through a double CE rather than a single CE before the first SN is that they contain stars of near-equal mass at ZAMS (Figure 2). Their stellar components evolve on similar timescales, which causes them to reach post–MS stages of evolution with expanded envelopes at around the same time. In POSYDON, if unstable MT is triggered and both stars are in RLO with a giant-like structure and core-envelope separation, the binary undergoes a double CE (Section 2.3).

After the first SN occurs and the NS is formed, the evolution for these binaries proceeds identically to those formed through Channel I, i.e. the evolution is fully detached and there is no MT onto the NS before the BH is formed.

### 3.3. NSBH DCO Properties

We plot the component masses at DCO formation for all NSBHs in our populations in Figure 5. The green and pink points represent the S16 population and the black points represent the F12d population. For the S16 population, the NSBHs are separated by their formation channels, with the pink points representing Channel I (Section 3.2.2) and the green points representing Channel II (Section 3.2.3). The F12d NSBHs do not need to be separated because all of them form through Channel I. The larger markers designate binaries that merge in a Hubble time, while the smaller markers represent binaries that remain detached.

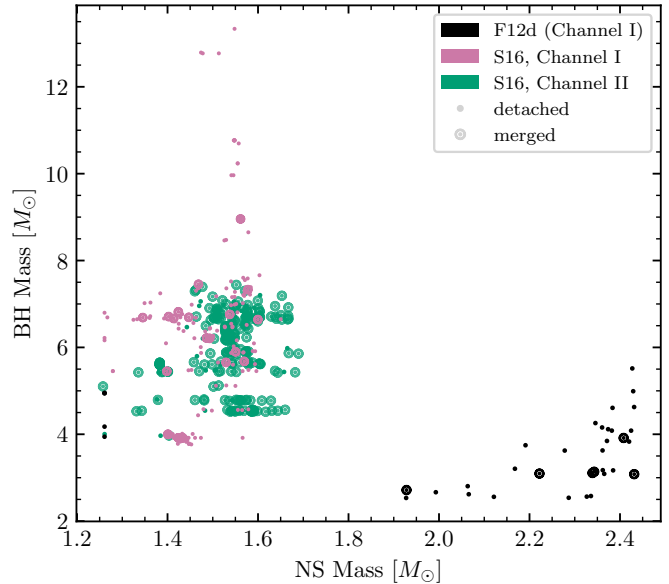


**Figure 5.** BH vs. NS masses for all NSBH binaries at their formation in both the F12d (black) and S16 (green/pink) populations. Each population is separated into binaries that merge and do not merge in a Hubble time with the large and small markers, respectively. For the S16 population, the NSBHs are also separated by Channel I vs. Channel II formation (Sections 3.2.2 & 3.2.3). All F12d NSBHs form through Channel I.

The most notable difference between the F12d and S16 NSBHs is the dominance of high-mass ( $> 2 M_{\odot}$ ) NSs in the F12d population. The F12d SN prescription will form NSs with masses up to the designated maximum NS mass limit (Fryer et al. 2012), which we set to  $2.5 M_{\odot}$ , whereas the S16 prescription does not form NS above about  $1.8 M_{\odot}$  (Sukhbold et al. 2016). Most of the F12d binaries with high-mass NSs have very low-mass BH companions ( $< 3 M_{\odot}$ ), implying their mass ratios remain close to unity even after both COs have formed. This is a consequence of the F12d SN mechanism, which produces more high-mass NS and low-mass BHs for NSBHs in general (see discussion in Section 3.1). However, we note that so far in the literature, the only explanation for the presence of low-mass BHs in GW sources and the existence of a low-end mass gap in X-ray binaries indicates that NS masses at birth may be limited to  $< 2 M_{\odot}$  like in the S16 prescription (Siegel et al. 2023).

There are a few low-mass NSs in both the F12d and S16 populations that have masses of  $1.26 M_{\odot}$ . All of these NSs formed through ECSNe. In POSYDON, the proto-NS mass is set uniformly for all stars undergoing ECSNe with the Podsiadlowski et al. (2004) prescription. The difference in modeling of ECSNe vs. CCSNe forms a gap in the NS masses for the F12d NSBHs.

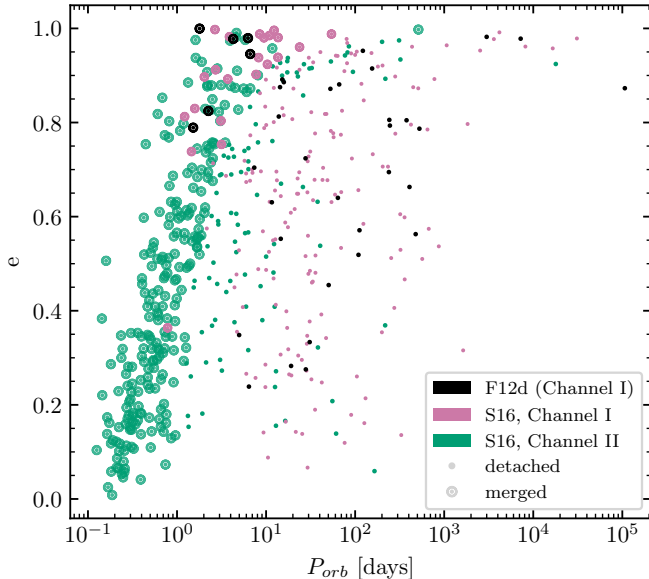


**Figure 6.** Eccentricity vs. orbital period for all NSBH binaries at their formation in both the F12d (black) and S16 (green/pink) populations. Each population is separated into binaries that merge and do not merge in a Hubble time with the large and small markers, respectively. For the S16 population, the NSBHs are also separated by Channel I vs. Channel II formation (Sections 3.2.2 & 3.2.3). All F12d NSBHs form through Channel I.

The S16 NSBH binaries have heavier BH components and a wider distribution of DCO mass ratios compared to the F12d binaries. As discussed in Section 3.1, this is because the type of CO formed from a given SN with the S16 mechanism is more stochastic than the F12d mechanism. Thus, even though these binaries may have ZAMS mass ratios close to one, this does not guarantee that the final DCO binary will also have a similar mass ratio. In addition, the S16 SN prescription does not produce BHs  $\lesssim 3.7 M_{\odot}$  or NSs  $\gtrsim 1.8 M_{\odot}$  with the N20 engine (Sukhbold et al. 2016), meaning there is a small gap between the heaviest NSs and lightest BHs that are formed.

We observe that the S16 NSBHs with the most unequal component masses (BHs  $> 8 M_{\odot}$ ) all form through Channel I. The Channel I systems can have more unequal ZAMS masses compared to the Channel II systems, which must have ZAMS mass ratios  $> 0.95$  in order to initiate the double CE phase (Sections 3.2.1 & 3.2.3).

In Figure 6, we plot the eccentricity vs. orbital period of all NSBHs in our populations. Similar to Figure 5, the green and pink points represent the S16 population and the black points represent the F12d population, while the two colors for the S16 NSBHs differentiate between

formation channels and the marker sizes distinguish between binaries that do and do not merge in a Hubble time.

For both the F12d and S16 populations, the merging NSBHs have shorter orbital periods than the detached NSBHs at DCO formation. This is especially true for the S16 Channel II systems, as they experience a double CE phase that significantly tightens the binary orbit before the first SN. Most of the mergers formed through Channel I in both the S16 and F12d populations have very high eccentricities with slightly greater orbital periods; the high eccentricity is necessary to merge these binaries in a Hubble time.

### 3.4. Model Variations

#### 3.4.1. Reduced CCSN Kicks

As mentioned in Section 2.4, we analyze the effects of reducing CCSN natal kicks by drawing kicks from a Maxwellian using the reduced kick scatter estimates from Mandel & Müller (2020). In this study, they predict a natal kick scatter of  $120 \text{ km s}^{-1}$  for NSs and  $60 \text{ km s}^{-1}$  for BHs formed via CCSN, which we set as the respective velocity dispersions for our Maxwellian kick distributions. These velocity dispersion estimates are greatly reduced compared to the scatter of  $265 \text{ km s}^{-1}$  for all NSs and BHs in our default models (Hobbs et al. 2005). Our adoption of the kick scatter estimates from Mandel & Müller (2020) does not consider their full kick model, which draws kicks from a Gaussian distribution centered at the normalized kick scatter values rather than a Maxwellian distribution.

In principle, we would expect reduced SN kicks to increase the number of bound NS–BH in our populations, as these systems are less likely to be disrupted upon CO formation. We find that this is indeed the case. Looking at Table 1, we see that the NSBH birth rate is an order of magnitude higher for the F12d population and over twice as high for the S16 population with the reduced kicks (designated as “low  $\sigma_{\text{CCSN}}$ ”). BHNSs still dominate the total NS–BH populations, and the birth rate for these systems is about four times higher for the F12d population and three times higher for the S16 population.

Qualitatively, all of the remaining results discussed in Section 3 are comparable between the NSBH populations formed with reduced CCSN kicks and our default kick settings. The primary mass distributions at ZAMS and the mass ratio distributions at ZAMS do not change for either the F12d or the S16 populations. The formation channels of NSBHs are the same, and the ratios of merged and detached binaries formed through Channel I and Channel II are comparable as well. Lastly, the

qualitative NSBH properties at DCO formation exhibit no significant changes between the model variation and the default.

### 3.4.2. *Reduced CE Efficiency*

The CE efficiency parameter  $\alpha$  (Section 2.3) impacts the “success” of the double CE events for NSBHs formed through Channel II. We set  $\alpha = 1$  in our default models, which is a relatively optimistic setting for allowing envelopes to be successfully ejected during CE. To evaluate the impact of  $\alpha$  on our results, we run two model variations with  $\alpha = 0.5$  and  $\alpha = 0.1$ , which we expect to make it more difficult for binaries to survive CE. We only run these model variations with the S16 remnant mass prescription because NSBHs formed through Channel II do not exist in the F12d population.

We find that changing the value of  $\alpha$  does not introduce any new possible formation channels for NSBHs, but lowering the value of  $\alpha$  “kills” most of the Channel II systems, which in turn lowers all NS–BH birth rates. We display the S16 birth rates with  $\alpha = 0.5$  and  $\alpha = 0.1$  in Table 1. In particular, the NSBH birth rate drops by about 62% when lowering  $\alpha$  from 1 to 0.5. As  $\alpha$  decreases, increasingly more potential NSBH progenitors do not survive the double CE phase and instead merge before the NS formation. We find that only 13% of NSBHs form through Channel II with  $\alpha = 0.5$  and no binaries form through Channel II with  $\alpha = 0.1$  (as opposed to 64% with  $\alpha = 1$ ). All of the  $\alpha = 0.5$  NSBHs that do form through Channel II merge in a Hubble time. This is expected, as decreasing  $\alpha$  also shrinks the separation of the binary after the envelope ejection (e.g., [Mapelli & Giacobbo 2018](#)).

The Channel I NSBH results do not change as  $\alpha$  is decreased, so the low- $\alpha$  S16 populations look approximately identical to Figures 3, 5, and 6 without the Channel II population present.

## 4. DISCUSSION

### 4.1. *Comparison with Previous Studies*

We present these results in conversation with previous studies that model BPS populations of NSBHs in the Milky Way, particularly as they relate to potential MSP–BH binaries. A recent study by [Chattopadhyay et al. \(2021\)](#) examines Galactic NS–BH populations using the COMPAS code ([Stevenson et al. 2017](#); [Vigna-Gómez et al. 2018](#); [Neijssel et al. 2019](#)). In contrast to our results, they find that COMPAS can produce populations of NSBHs with recycled NSs, allowing for the presence of a detectable Galactic MSP–BH population. The dominant formation channel for these systems is as follows: the initially more massive primary initiates

stable MT onto the secondary during the HMS–HMS evolution and then eventually explodes to form a NS. The secondary then also expands to fill its Roche lobe, which initiates unstable MT and a CE phase that facilitates significant accretion onto the NS. If the CE is successful, the binary orbit dramatically shrinks and an instance of stable Case BB MT phase may occur before the second SN, depending on the mass of the secondary star. These MT phases after the first SN, particularly the MT during CE, are required to obtain MSP populations in COMPAS that are consistent with Galactic double NS observations ([Chattopadhyay et al. 2021](#)).

In COMPAS, CE initiation after the NS formation is possible due to their treatment of stable MT, which leads to the formation of NS–BH binaries with asymmetric masses in their populations ([Broekgaarden et al. 2021](#)). Their MT prescription allows for more efficient accretion during the HMS–HMS evolution than the MT treatment in POSYDON’s pre-computed MESA models, as stellar accretion in COMPAS is only constrained by the thermal timescales of the donor and the accretor and does not consider the accretor’s rotation rate ([Stevenson et al. 2017](#)). As a result, [Chattopadhyay et al. \(2021\)](#) find that the first episode of MT is almost completely conservative for NS–BH progenitors, which in their model means that all the mass lost by the donor is successfully accreted by the companion. This implies that mass ratio reversal can happen for more asymmetric ZAMS masses. Because the progenitor stars are evolving on different timescales in this case, a single CE after the first SN is allowed to take place.

In contrast, mass accretion onto non-degenerate companions in POSYDON is limited by the critical rotation rate of the accretor, as discussed in Section 2.2 ([Fragos et al. 2023](#)). This means that the actual amount of mass accreted by the secondary may be very low depending on its angular momentum and stellar structure, even when assuming initially conservative MT between the donor and accretor. Such a scenario is not uncommon, as non-degenerate accretors will gain angular momentum and can often reach critical rotation rates during MT. The result of this is that mass ratio reversal during HMS–HMS evolution only occurs for binaries with ZAMS mass ratios near unity, and potential NSBH progenitors with more unequal masses are disrupted (Section 3.2).

It is important to note that [Chattopadhyay et al. \(2021\)](#) find infrequent instances of NSBH formation nearly identical to our Channel II binaries. For COMPAS NS–BH binaries with ZAMS mass ratios very close to one, the stars evolve on similar timescales, which causes them to enter a double CE phase before the first SN.

Because the NS now forms after the CE, it does not undergo any mass accretion and thus BH binaries with recycled NSs do not form. In this case, our results are in agreement with one another.

The study done by Kruckow et al. (2018) examines Galactic DCO populations with the ComBinE code (Tauris & Bailes 1996; Voss & Tauris 2003). When looking at NSBH formation channels, they find that no CE or stable MT occurs after the first SN, and thus recycled NSs with BH companions do not form at all in their populations. They do not treat double CE evolution, so all of their NSBHs form through our Channel I evolution. The key to this result is that they assume highly inefficient MT, which, like in our study, requires their NSBH progenitors to have near-equal ZAMS masses for mass ratio reversal to occur during the HMS–HMS evolution (Kruckow et al. 2018). In this sense, our results are in agreement with one another. However, while they make the inefficient MT assumption in efforts to better match their populations to double NS observations, it is important to note that their findings are sensitive to this fine-tuned setting of MT parameters, while in POSYDON the MT is more robustly and self-consistently handled by the pre-computed MESA models.

#### 4.2. Model Uncertainties

As discussed throughout Section 3, our results are most impacted by the CC prescription used in our BPS models. Changing this prescription between F12d and S16 impacts the NS–BH birth rate by multiple orders of magnitude (Table 1). In addition, it determines the possible NSBH formation channels (Section 3.2.3), which not only controls the (absence of) recycled NSs, but also affects the NSBH DCO properties (Figures 5 & 6). Chattopadhyay et al. (2021) also find that the birth rates and properties of NS–BHs change significantly when comparing different SN remnant mass prescriptions. For example, they report the total NS–BH birth rate is over twice as high for populations run with the Fryer–12 rapid prescription compared to the Fryer–12 delayed prescription, and the ZAMS mass ratios of the rapid NSBHs are significantly lower than those of the delayed NSBHs. This further confirms that the formation rates, channels, and properties of NSBHs are very sensitive to how remnant masses and remnant types are determined, which makes sense given that these systems require relatively specific pre-SN conditions to form successfully. Thus, future CC prescriptions could potentially introduce new NSBH formation channels not identified in this paper and change the NSBH population properties.

We also reiterate the model uncertainties related to double CE evolution discussed in Section 2.3. The phys-

ical conditions that lead to the onset of a double CE are thought to differ from those for a single CE because MT is not expected to become unstable in the same manner for post-MS stars of near-equal mass (Ivanova et al. 2020). In POSYDON, we assume that all binaries with two components in RLO that contain at least one post-MS stellar component immediately initiate unstable MT, and this condition in particular could lead to an over-estimation of the number of binaries undergoing double CE in our populations. The amount of double CE NSBHs is also sensitive to the MT classification performed by POSYDON’s initial-final interpolation scheme, as most of the double CE systems lie on a classification boundary in the HMS–HMS grids (Section 3.2.1). Improvements in the classification method could change how many NSBHs go through a double CE phase.

NSBH formation is impacted by the He-burning stars that serve as NS companions before the second SN (Section 3.2.2). The behavior of these stars in relation to the binary orbit primarily determines if MT onto the NS will occur or not. Changes in the related input physics of the pre-computed MESA models, such as the stellar wind scheme used for these He stars, could potentially affect our results. Changing stellar winds would not only impact the total amount of stellar mass-loss, but could also change the orbital separation of the binary. Currently, stellar winds for high-mass stars ( $> 8 M_{\odot}$ ) in POSYDON are treated using the MESA Dutch scheme, which captures key features of massive stellar evolution (Fragos et al. 2023).

In addition, the method of assigning binary properties from the MESA grids during BPS can impact the resulting populations. We use POSYDON’s initial-final interpolation scheme in all of our binary populations (Section 2). To assess potential uncertainties due to this choice of interpolator, we also run populations using POSYDON’s nearest-neighbor scheme for acquiring binary properties (Fragos et al. 2023; Andrews et al. 2024). We find that our qualitative results, such as the distinct NSBH formation channels, do not change when assigning binary properties with nearest-neighbor instead of initial-final interpolation. We find that our quantitative results with nearest-neighbor, such as the birth rate of NSBHs, scale in a similar manner as when lowering the SN kicks.

Lastly, our results are sensitive to the resolution of POSYDON’s pre-computed grids as well as the presence of unconverged MESA models in these grids. An increased grid resolution will improve the accuracy of the binary MT classification and the interpolation of binary properties.

#### 4.3. Implications for MSP–BH Detections

As discussed in Section 1, only one possible MSP–BH system has been detected thus far; the companion object falls in the lower mass gap and cannot be differentiated between a low-mass BH and high-mass NS (Barr et al. 2024). Because of its location in the globular cluster NGC 1851, it is predicted that this system formed dynamically, where the MSP was first spun-up by a low-mass companion that was later replaced by a high-mass companion through exchange interactions (Barr et al. 2024). Theoretical models predict that it is relatively difficult to form NS–BH systems in GCs (e.g., Clausen et al. 2014; Ye et al. 2019a; Arca Sedda 2020; Hoang et al. 2020), but MSP formation is thought to be more efficient in these environments (e.g., Manchester et al. 2005; Ransom 2008; Bahramian et al. 2013). Ye et al. (2019b) find that the number of MSPs in a given cluster may even be anti-correlated with the number of BHs, making MSP–BH formation unlikely.

Other potential formation environments could include active galactic nuclei (AGN) such as the Galactic center (e.g., Fragione et al. 2019; Stephan et al. 2019; McKernan et al. 2020) or isolated stellar triples (e.g., Toonen et al. 2016; Liu & Lai 2018; Fragione & Loeb 2019), both of which allow for more complex channels of NS–BH formation. However, the formation of MSP–BH binaries in these environments has not been studied in detail.

Past BPS studies have examined the formation of isolated NSBHs in Milky Way-like galaxies, but come to opposing conclusions regarding the ability of these systems to recycle NSs (Kruckow et al. 2018; Chattopadhyay et al. 2021). We find that while NSBHs can form in the Galactic field, the pulsars in these binaries will not be recycled.

With all of this in consideration, our results have important implications for current and future pulsar surveys targeting pulsar–BH systems. If surveys wish to observe a MSP–BH system specifically, it is more likely that this will happen by targeting dynamically active environments (such as Galactic GCs or nuclear clusters). However, we cannot assess the uncertainties related to NSBH formation or observations in these environments in the current study.

## 5. CONCLUSIONS

We simulate populations of binaries at solar metallicity using the POSYDON population synthesis code and examine the properties of the NS–BH subpopulation, including both merged and detached systems. We find that NS–BH binaries in which the NS forms first (NS–BHs) are significantly less common than those where the BH forms first (BHNSs). The Galactic birth rate of NSBHs is highly dependent on the CC prescription,

kick prescription, and CE efficiency parameter  $\alpha$  used in modeling the binary population. For example, we find that the birth rate of NSBHs is about an order of magnitude higher with the S16 remnant mass prescription compared to the F12d prescription, and these differences are even greater when lowering CCSN kicks but diminish when reducing the value of  $\alpha$ .

All NSBHs in our populations have ZAMS mass ratios close to unity, and all of them undergo a mass ratio reversal before the first SN via MT during HMS–HMS evolution. The mass accretion of the secondary during HMS–HMS evolution is relatively inefficient due to POSYDON’s treatment of rotationally-limited accretion and boosted stellar winds. After the first SN, NSBHs form through two different channels. In Channel I, the binary undergoes fully detached evolution after the HMS–HMS phase, all the way through the second SN. In Channel II, the binary experiences a double CE phase of evolution after the HMS–HMS phase and before the first SN. In both cases, there is no MT, stable or unstable, in the binary after the first SN.

The lack of MT after the first SN implies that there is no possibility of accretion onto the NS in our NSBH binaries. Accretion is required to recycle the NS, and thus we conclude that MSP–BH binaries cannot be formed. We suggest that ongoing pulsar surveys are more likely to detect these systems in dynamically active environments in the Milky Way.

## ACKNOWLEDGEMENTS

The authors thank Debatri Chattopadhyay and Chase Kimball for their input on our methods and results. C.L. and V.K. acknowledge support from the Gordon and Betty Moore Foundation (grant awards GBMF8477 and GBMF12341), CIERA, and Northwestern University. V.K. was partially supported through the D.I.Linzer Distinguished University Professorship fund. P.M.S., E.T., K.A.R., M.S., and S.G. were also supported by the project numbers GBMF8477 and GBMF12341. J.J.A. acknowledges support for program number JWST-AR-04369.001-A provided through a grant from the STScI under NASA contract NAS5-03127. S.S.B., T.F., M.U.K., and Z.X. were supported by the the Swiss National Science Foundation, project number PP00P2.211006. S.S.B. and M.M.B. were supported by the the Swiss National Science Foundation, project number CRSII5\_213497. M.M.B. is also supported by the Boninchi Foundation and the Swiss Government Excellence Scholarship. K.K. is supported by a fellowship program at the Institute of Space Sciences (ICE-CSIC) funded by the program Unidad de Excelencia María de Maeztu CEX2020-001058-M. Z.X. ac-

knowledges support from the Chinese Scholarship Council (CSC). E.Z. acknowledges support from the Hellenic Foundation for Research and Innovation (H.F.R.I.) under the “3rd Call for H.F.R.I. Research Projects to support Post-Doctoral Researchers” (Project No: 7933). The computations were performed at Northwestern University on the Trident computer cluster (funded by the GBMF8477 award) and at the University of Geneva on the Yggdrasil computer cluster. This research

was partly supported by the computational resources and staff contributions provided for the Quest high-performance computing facility at Northwestern University, jointly supported by the Office of the Provost, the Office for Research and Northwestern University Information Technology.

*Software:* POSYDON (Fragos et al. 2023; Andrews et al. 2024); Matplotlib (Hunter 2007); NumPy (van der Walt et al. 2011); Pandas (McKinney 2010).

## REFERENCES

- Abac, A. G., Abbott, R., Abouelfettouh, I., et al. 2024, *The Astrophysical Journal Letters*, 970, L34, doi: [10.3847/2041-8213/ad5beb](https://doi.org/10.3847/2041-8213/ad5beb)
- Abbott, R., Abbott, T. D., Abraham, S., et al. 2020, *The Astrophysical Journal Letters*, 896, L44, doi: [10.3847/2041-8213/ab960f](https://doi.org/10.3847/2041-8213/ab960f)
- . 2021, *The Astrophysical Journal Letters*, 915, L5, doi: [10.3847/2041-8213/ac082e](https://doi.org/10.3847/2041-8213/ac082e)
- Abbott, R., Abbott, T., Acernese, F., et al. 2023, *Physical Review X*, 13, 041039, doi: [10.1103/PhysRevX.13.041039](https://doi.org/10.1103/PhysRevX.13.041039)
- Abbott, R., Abbott, T. D., Acernese, F., et al. 2024, *Physical Review D*, 109, 022001, doi: [10.1103/PhysRevD.109.022001](https://doi.org/10.1103/PhysRevD.109.022001)
- Ahmad, A., Jeffery, C. S., & Fullerton, A. W. 2004, *Astronomy and Astrophysics*, 418, 275, doi: [10.1051/0004-6361:20035917](https://doi.org/10.1051/0004-6361:20035917)
- Amiri, M., Bandura, K. M., Boyle, P. J., et al. 2021, *The Astrophysical Journal Supplement Series*, 255, 5, doi: [10.3847/1538-4365/abfdcb](https://doi.org/10.3847/1538-4365/abfdcb)
- Andrews, J. J., Bavera, S. S., Briel, M., et al. 2024, POSYDON Version 2: Population Synthesis with Detailed Binary-Evolution Simulations across a Cosmological Range of Metallicities, arXiv, doi: [10.48550/arXiv.2411.02376](https://doi.org/10.48550/arXiv.2411.02376)
- Arca Sedda, M. 2020, *Communications Physics*, 3, 1, doi: [10.1038/s42005-020-0310-x](https://doi.org/10.1038/s42005-020-0310-x)
- Bahramian, A., Heinke, C. O., Sivakoff, G. R., & Gladstone, J. C. 2013, *The Astrophysical Journal*, 766, 136, doi: [10.1088/0004-637X/766/2/136](https://doi.org/10.1088/0004-637X/766/2/136)
- Barr, E. D., Dutta, A., Freire, P. C. C., et al. 2024, *Science*, 383, 275, doi: [10.1126/science.adg3005](https://doi.org/10.1126/science.adg3005)
- Booth, R. S., de Blok, W. J. G., Jonas, J. L., & Fanaroff, B. 2009, MeerKAT Key Project Science, Specifications, and Proposals, arXiv, doi: [10.48550/arXiv.0910.2935](https://doi.org/10.48550/arXiv.0910.2935)
- Branchesi, M. 2023, in *Bruno Touschek 100 Years*, ed. L. Bonolis, L. Maiani, & G. Pancheri (Cham: Springer International Publishing), 255–266, doi: [10.1007/978-3-031-23042-4\\_19](https://doi.org/10.1007/978-3-031-23042-4_19)
- Braun, R., Bonaldi, A., Bourke, T., Keane, E., & Wagg, J. 2019, Anticipated Performance of the Square Kilometre Array – Phase 1 (SKA1), arXiv, doi: [10.48550/arXiv.1912.12699](https://doi.org/10.48550/arXiv.1912.12699)
- Broekgaarden, F. S., Berger, E., Neijssel, C. J., et al. 2021, *Monthly Notices of the Royal Astronomical Society*, 508, 5028, doi: [10.1093/mnras/stab2716](https://doi.org/10.1093/mnras/stab2716)
- Chattopadhyay, D., Stevenson, S., Hurley, J. R., Bailes, M., & Broekgaarden, F. 2021, *Monthly Notices of the Royal Astronomical Society*, 504, 3682, doi: [10.1093/mnras/stab973](https://doi.org/10.1093/mnras/stab973)
- Clausen, D., Sigurdsson, S., & Chernoff, D. F. 2013, *Monthly Notices of the Royal Astronomical Society*, 428, 3618, doi: [10.1093/mnras/sts295](https://doi.org/10.1093/mnras/sts295)
- . 2014, *Monthly Notices of the Royal Astronomical Society*, 442, 207, doi: [10.1093/mnras/stu871](https://doi.org/10.1093/mnras/stu871)
- Colpi, M., Nannurelli, M., & Calvani, M. 1991, *Monthly Notices of the Royal Astronomical Society*, 253, 55, doi: [10.1093/mnras/253.1.55](https://doi.org/10.1093/mnras/253.1.55)
- D’Antona, F., & Tailo, M. 2020, Origin and binary evolution of millisecond pulsars, arXiv, doi: [10.48550/arXiv.2011.11385](https://doi.org/10.48550/arXiv.2011.11385)
- Drozda, P., Belczynski, K., O’Shaughnessy, R., Bulik, T., & Fryer, C. L. 2022, *Astronomy & Astrophysics*, 667, A126, doi: [10.1051/0004-6361/202039418](https://doi.org/10.1051/0004-6361/202039418)
- Fonseca, E., Demorest, P., Ransom, S., & Stairs, I. 2019, *Bulletin of the AAS*, 51, <https://baas.aas.org/pub/2020n3i425/release/1>
- Fragione, G., & Banerjee, S. 2020, *The Astrophysical Journal Letters*, 901, L16, doi: [10.3847/2041-8213/abb671](https://doi.org/10.3847/2041-8213/abb671)
- Fragione, G., Grishin, E., Leigh, N. W. C., Perets, H. B., & Perna, R. 2019, *Monthly Notices of the Royal Astronomical Society*, 488, 47, doi: [10.1093/mnras/stz1651](https://doi.org/10.1093/mnras/stz1651)
- Fragione, G., & Loeb, A. 2019, *Monthly Notices of the Royal Astronomical Society*, 486, 4443, doi: [10.1093/mnras/stz1131](https://doi.org/10.1093/mnras/stz1131)

- Fragos, T., Andrews, J. J., Bavera, S. S., et al. 2023, *The Astrophysical Journal Supplement Series*, 264, 45, doi: [10.3847/1538-4365/ac90c1](https://doi.org/10.3847/1538-4365/ac90c1)
- Fryer, C. L., Belczynski, K., Wiktorowicz, G., et al. 2012, *The Astrophysical Journal*, 749, 91, doi: [10.1088/0004-637X/749/1/91](https://doi.org/10.1088/0004-637X/749/1/91)
- Giacobbo, N., & Mapelli, M. 2019, *Monthly Notices of the Royal Astronomical Society*, 482, 2234, doi: [10.1093/mnras/sty2848](https://doi.org/10.1093/mnras/sty2848)
- Habets, G. M. H. J. 1986, *Astronomy and Astrophysics*, 167, 61, <https://ui.adsabs.harvard.edu/abs/1986A&A...167...61H>
- Hiramatsu, D., Howell, D. A., Van Dyk, S. D., et al. 2021, *Nature Astronomy*, 5, 903, doi: [10.1038/s41550-021-01384-2](https://doi.org/10.1038/s41550-021-01384-2)
- Hoang, B.-M., Naoz, S., & Kremer, K. 2020, *The Astrophysical Journal*, 903, 8, doi: [10.3847/1538-4357/abb66a](https://doi.org/10.3847/1538-4357/abb66a)
- Hobbs, G., Lorimer, D. R., Lyne, A. G., & Kramer, M. 2005, *Monthly Notices of the Royal Astronomical Society*, 360, 974, doi: [10.1111/j.1365-2966.2005.09087.x](https://doi.org/10.1111/j.1365-2966.2005.09087.x)
- Hunter, J. D. 2007, *Computing in Science & Engineering*, 9, 90, doi: [10.1109/MCSE.2007.55](https://doi.org/10.1109/MCSE.2007.55)
- Ivanova, N., Justham, S., & Ricker, P. 2020, *Common Envelope Evolution* (IOP Publishing). <https://iopscience.iop.org/book/mono/978-0-7503-1563-0>
- Justham, S., Podsiadlowski, P., & Han, Z. 2011, *Monthly Notices of the Royal Astronomical Society*, 410, 984, doi: [10.1111/j.1365-2966.2010.17497.x](https://doi.org/10.1111/j.1365-2966.2010.17497.x)
- Kolb, U., & Ritter, H. 1990, *Astronomy and Astrophysics*, 236, 385, <https://ui.adsabs.harvard.edu/abs/1990A&A...236..385K>
- Kramer, M., Backer, D. C., Cordes, J. M., et al. 2004, *New Astronomy Reviews*, 48, 993, doi: [10.1016/j.newar.2004.09.020](https://doi.org/10.1016/j.newar.2004.09.020)
- Kroupa, P. 2001, *Monthly Notices of the Royal Astronomical Society*, 322, 231, doi: [10.1046/j.1365-8711.2001.04022.x](https://doi.org/10.1046/j.1365-8711.2001.04022.x)
- Kruckow, M. U., Tauris, T. M., Langer, N., Kramer, M., & Izzard, R. G. 2018, *Monthly Notices of the Royal Astronomical Society*, 481, 1908, doi: [10.1093/mnras/sty2190](https://doi.org/10.1093/mnras/sty2190)
- Lazarus, P., Tauris, T. M., Knispel, B., et al. 2014, *Monthly Notices of the Royal Astronomical Society*, 437, 1485, doi: [10.1093/mnras/stt1996](https://doi.org/10.1093/mnras/stt1996)
- Licquia, T. C., & Newman, J. A. 2015, *The Astrophysical Journal*, 806, 96, doi: [10.1088/0004-637X/806/1/96](https://doi.org/10.1088/0004-637X/806/1/96)
- Liu, B., & Lai, D. 2018, *The Astrophysical Journal*, 863, 68, doi: [10.3847/1538-4357/aad09f](https://doi.org/10.3847/1538-4357/aad09f)
- Livio, M., & Soker, N. 1988, *The Astrophysical Journal*, 329, 764, doi: [10.1086/166419](https://doi.org/10.1086/166419)
- Lorimer, D. R. 2008, *Living Reviews in Relativity*, 11, 8, doi: [10.12942/lrr-2008-8](https://doi.org/10.12942/lrr-2008-8)
- Manchester, R. N., Hobbs, G. B., Teoh, A., & Hobbs, M. 2005, *The Astronomical Journal*, 129, 1993, doi: [10.1086/428488](https://doi.org/10.1086/428488)
- Mandel, I., & Müller, B. 2020, *Monthly Notices of the Royal Astronomical Society*, 499, 3214, doi: [10.1093/mnras/staa3043](https://doi.org/10.1093/mnras/staa3043)
- Mapelli, M., & Giacobbo, N. 2018, *Monthly Notices of the Royal Astronomical Society*, 479, 4391, doi: [10.1093/mnras/sty1613](https://doi.org/10.1093/mnras/sty1613)
- McKernan, B., Ford, K. E. S., & O’Shaughnessy, R. 2020, *Monthly Notices of the Royal Astronomical Society*, 498, 4088, doi: [10.1093/mnras/staa2681](https://doi.org/10.1093/mnras/staa2681)
- McKinney, W. 2010, in *Proceedings of the 9th Python in Science Conference*, 56–61, doi: [10.25080/Majora-92bf1922-00a](https://doi.org/10.25080/Majora-92bf1922-00a)
- Mészáros, P., Fox, D. B., Hanna, C., & Murase, K. 2019, *Nature Reviews Physics*, 1, 585, doi: [10.1038/s42254-019-0101-z](https://doi.org/10.1038/s42254-019-0101-z)
- Nan, R., Li, D., Jin, C., et al. 2011, *International Journal of Modern Physics D*, 20, 989, doi: [10.1142/S0218271811019335](https://doi.org/10.1142/S0218271811019335)
- Neijssel, C. J., Vigna-Gómez, A., Stevenson, S., et al. 2019, *Monthly Notices of the Royal Astronomical Society*, 490, 3740, doi: [10.1093/mnras/stz2840](https://doi.org/10.1093/mnras/stz2840)
- Nomoto, K. 1984, *The Astrophysical Journal*, 277, 791, doi: [10.1086/161749](https://doi.org/10.1086/161749)
- Paczynski, B. 1976, 73, 75, <http://adsabs.harvard.edu/abs/1976IAUS...73...75P>
- . 1991, *The Astrophysical Journal*, 370, 597, doi: [10.1086/169846](https://doi.org/10.1086/169846)
- Paxton, B., Bildsten, L., Dotter, A., et al. 2011, *The Astrophysical Journal Supplement Series*, 192, 3, doi: [10.1088/0067-0049/192/1/3](https://doi.org/10.1088/0067-0049/192/1/3)
- Paxton, B., Cantiello, M., Arras, P., et al. 2013, *The Astrophysical Journal Supplement Series*, 208, 4, doi: [10.1088/0067-0049/208/1/4](https://doi.org/10.1088/0067-0049/208/1/4)
- Paxton, B., Marchant, P., Schwab, J., et al. 2015, *The Astrophysical Journal Supplement Series*, 220, 15, doi: [10.1088/0067-0049/220/1/15](https://doi.org/10.1088/0067-0049/220/1/15)
- Paxton, B., Smolec, R., Schwab, J., et al. 2019, *The Astrophysical Journal Supplement Series*, 243, 10, doi: [10.3847/1538-4365/ab2241](https://doi.org/10.3847/1538-4365/ab2241)
- Peters, P. C. 1964, *Physical Review*, 136, B1224, doi: [10.1103/PhysRev.136.B1224](https://doi.org/10.1103/PhysRev.136.B1224)

- Phinney, E. S., & Kulkarni, S. R. 1994, *Annual Review of Astronomy and Astrophysics*, 32, 591, doi: [10.1146/annurev.aa.32.090194.003111](https://doi.org/10.1146/annurev.aa.32.090194.003111)
- Podsiadlowski, P., Langer, N., Poelarends, A. J. T., et al. 2004, *The Astrophysical Journal*, 612, 1044, doi: [10.1086/421713](https://doi.org/10.1086/421713)
- Popham, R., & Narayan, R. 1991, *The Astrophysical Journal*, 370, 604, doi: [10.1086/169847](https://doi.org/10.1086/169847)
- Ransom, S. M. 2008, 246, 291, doi: [10.1017/S1743921308015810](https://doi.org/10.1017/S1743921308015810)
- Román-Garza, J., Bavera, S. S., Fragos, T., et al. 2021, *The Astrophysical Journal Letters*, 912, L23, doi: [10.3847/2041-8213/abf42c](https://doi.org/10.3847/2041-8213/abf42c)
- Sana, H., de Mink, S. E., de Koter, A., et al. 2012, *Science*, 337, 444, doi: [10.1126/science.1223344](https://doi.org/10.1126/science.1223344)
- Seymour, B., & Yagi, K. 2018, *Physical Review D*, 98, 124007, doi: [10.1103/PhysRevD.98.124007](https://doi.org/10.1103/PhysRevD.98.124007)
- Shao, Y., & Li, X.-D. 2018, *Monthly Notices of the Royal Astronomical Society: Letters*, 477, L128, doi: [10.1093/mnrasl/sly063](https://doi.org/10.1093/mnrasl/sly063)
- Shapiro, I. I. 1964, *Physical Review Letters*, 13, 789, doi: [10.1103/PhysRevLett.13.789](https://doi.org/10.1103/PhysRevLett.13.789)
- Siegel, J. C., Kiato, I., Kalogera, V., et al. 2023, *The Astrophysical Journal*, 954, 212, doi: [10.3847/1538-4357/ace9d9](https://doi.org/10.3847/1538-4357/ace9d9)
- Stairs, I. 2019, 233, 110.02. <https://ui.adsabs.harvard.edu/abs/2019AAS...23311002S>
- Stephan, A. P., Naoz, S., Ghez, A. M., et al. 2019, *The Astrophysical Journal*, 878, 58, doi: [10.3847/1538-4357/ab1e4d](https://doi.org/10.3847/1538-4357/ab1e4d)
- Stevenson, S., Vigna-Gómez, A., Mandel, I., et al. 2017, *Nature Communications*, 8, 14906, doi: [10.1038/ncomms14906](https://doi.org/10.1038/ncomms14906)
- Sukhbold, T., Ertl, T., Woosley, S. E., Brown, J. M., & Janka, H.-T. 2016, *The Astrophysical Journal*, 821, 38, doi: [10.3847/0004-637X/821/1/38](https://doi.org/10.3847/0004-637X/821/1/38)
- Tauris, T. M., & Bailes, M. 1996, *Astronomy and Astrophysics*, 315, 432. <https://ui.adsabs.harvard.edu/abs/1996A&A...315..432T>
- Tauris, T. M., Langer, N., & Kramer, M. 2012, *Monthly Notices of the Royal Astronomical Society*, 425, 1601, doi: [10.1111/j.1365-2966.2012.21446.x](https://doi.org/10.1111/j.1365-2966.2012.21446.x)
- Tauris, T. M., Langer, N., & Podsiadlowski, P. 2015, *Monthly Notices of the Royal Astronomical Society*, 451, 2123, doi: [10.1093/mnras/stv990](https://doi.org/10.1093/mnras/stv990)
- Tauris, T. M., Kramer, M., Freire, P. C. C., et al. 2017, *The Astrophysical Journal*, 846, 170, doi: [10.3847/1538-4357/aa7e89](https://doi.org/10.3847/1538-4357/aa7e89)
- Toonen, S., Hamers, A., & Portegies Zwart, S. 2016, *Computational Astrophysics and Cosmology*, 3, 6, doi: [10.1186/s40668-016-0019-0](https://doi.org/10.1186/s40668-016-0019-0)
- van der Walt, S., Colbert, S. C., & Varoquaux, G. 2011, *Computing in Science & Engineering*, 13, 22, doi: [10.1109/MCSE.2011.37](https://doi.org/10.1109/MCSE.2011.37)
- Vigna-Gómez, A., Neijssel, C. J., Stevenson, S., et al. 2018, *Monthly Notices of the Royal Astronomical Society*, 481, 4009, doi: [10.1093/mnras/sty2463](https://doi.org/10.1093/mnras/sty2463)
- Voss, R., & Tauris, T. M. 2003, *Monthly Notices of the Royal Astronomical Society*, 342, 1169, doi: [10.1046/j.1365-8711.2003.06616.x](https://doi.org/10.1046/j.1365-8711.2003.06616.x)
- Webbink, R. F. 1984, *The Astrophysical Journal*, 277, 355, doi: [10.1086/161701](https://doi.org/10.1086/161701)
- Xing, Z., Bavera, S. S., Fragos, T., et al. 2023, *From ZAMS to Merger: Detailed Binary Evolution Models of Coalescing Neutron Star-Black Hole Systems at Solar Metallicity*, arXiv, doi: [10.48550/arXiv.2309.09600](https://doi.org/10.48550/arXiv.2309.09600)
- Xing, Z., Kalogera, V., Fragos, T., et al. 2024, *Mass-gap Black Holes in Coalescing Neutron Star Black Hole Binaries*, arXiv, doi: [10.48550/arXiv.2410.20415](https://doi.org/10.48550/arXiv.2410.20415)
- Ye, C. S., Fong, W.-f., Kremer, K., et al. 2019a, *The Astrophysical Journal Letters*, 888, L10, doi: [10.3847/2041-8213/ab5dc5](https://doi.org/10.3847/2041-8213/ab5dc5)
- Ye, C. S., Kremer, K., Chatterjee, S., Rodriguez, C. L., & Rasio, F. A. 2019b, *The Astrophysical Journal*, 877, 122, doi: [10.3847/1538-4357/ab1b21](https://doi.org/10.3847/1538-4357/ab1b21)
- Şener, H. T., & Jeffery, C. S. 2014, *Monthly Notices of the Royal Astronomical Society*, 440, 2676, doi: [10.1093/mnras/stu397](https://doi.org/10.1093/mnras/stu397)